Synthesis, structural, and transport properties of the hole-doped superconductor $Pr_{1-x}Sr_xFeAsO$

Gang Mu, Bin Zeng, Xiyu Zhu, Fei Han, Peng Cheng, Bing Shen, and Hai-Hu Wen*
National Laboratory for Superconductivity, Institute of Physics and Beijing National Laboratory for Condensed Matter, Chinese Academy of Sciences, P.O. Box 603, Beijing 100190, People's Republic of China
(Received 9 October 2008; revised manuscript received 13 January 2009; published 3 March 2009)

Superconductivity was achieved in PrFeAsO by partially substituting Pr^{3+} with Sr^{2+}. The electrical transport properties and structure of this superconductor $Pr_{1-x}Sr_xFeAsO$ at different doping levels ($x=0.05\sim0.25$) were investigated systematically. It was found that the lattice constants (a and c axes) increase monotonously with Sr or hole concentration. The superconducting transition temperature at about 16.3 K (95% ρ_n) was observed around the doping level of $0.20\sim0.25$. A detailed investigation was carried out in the sample with doping level of $x=0.25$. The domination of holelike charge carriers in this material was confirmed by Hall-effect measurements. The magnetoresistance (MR) behavior can be well described by a simple two-band model. The upper critical field of the sample with $T_c=16.3$ K ($x=0.25$) was estimated to be beyond 45 T. Our results suggest that the hole-doped samples may have higher upper critical fields comparing to the electron-doped ones, due to the higher quasiparticle density of states at the Fermi level.

DOI: 10.1103/PhysRevB.79.104501 PACS number(s): 74.10.+v, 74.25.Fy, 74.62.Dh, 74.25.Dw

I. INTRODUCTION

The discovery of superconductivity at 26 K in FeAs-based layered quaternary compound $LaFeAsO_{1-x}F_x$ has attracted great interest in the fields of condensed-matter physics and material sciences.[1,2] The family of the FeAs-based superconductors has been extended rapidly and it can be divided into three categories. The first category has the general formula of REFeAsO where RE stands for the rare-earth elements and is abbreviated as the FeAs-1111 phase.[3] The second class is formulated as $(Ba,Sr)_{1-x}K_xFe_2As_2$ which is denoted as FeAs-122 for simplicity.[4,5] The third type Li_xFeAs has an infinite layered structure (denoted as FeAs-111).[6–8] As for the FeAs-1111 phase, most of the discovered superconductors are characterized as electron doped ones and the superconducting transition temperature has been quickly raised to $T_c=55\sim56$ K via replacing lanthanum with other rare-earth elements.[9–14] About the hole-doped side, however, since the first hole-doped superconductor $La_{1-x}Sr_xFeAsO$ with $T_c\approx25$ K was discovered,[15,16] only the Nd-based system $Nd_{1-x}Sr_xFeAsO$ with $T_c=13.5$ K was reported.[17] Obviously, there is an extensive space to explore more superconductors in the hole-doped side based on the FeAs-1111 phase and to further extend the family of the FeAs-based superconductors. Moreover it is also significant to investigate the basic physical properties of the hole-doped system based on the FeAs-1111 phase.

In this paper we report a new route to easily synthesize the hole-doped superconductors based on the FeAs-1111 phase, Sr doped $Pr_{1-x}Sr_xFeAsO$, with the maximum superconducting transition temperature of 16.3 K. We carried out a systematic study on the evolution of the superconductivity and the lattice constants with the content of Sr or hole concentration in the system of $Pr_{1-x}Sr_xFeAsO$. We found that the a and c axes lattice constants increase monotonously with doped concentration of Sr or hole numbers. The physical properties of a selected sample with $x=0.25$ were investigated in depth. The conducting charge carriers in this sample were characterized to be hole type by the Hall-effect measurements. Moreover, it is found that the MR data show a good two-band behavior. We also estimated the upper critical field of the same sample based on the Ginzburg-Landau theory as well as the Werthamer-Helfand-Hohenberg (WHH) formula.[18] It is suggested that the upper critical fields in the hole-doped samples may be higher than that in the electron-doped ones.

II. EXPERIMENTAL DETAILS

The $Pr_{1-x}Sr_xFeAsO$ samples were prepared using a two-step solid-state reaction method. In the first step, PrAs and SrAs were prepared by reacting Pr flakes (purity 99.99%), Sr flakes (purity 99.9%), and As grains (purity 99.99%) at 500 °C for 8 h and then 700 °C for 16 h. They were sealed in an evacuated quartz tube when reacting. Then the resultant precursors were thoroughly ground together with Fe powder (purity 99.95%) and Fe_2O_3 powder (purity 99.5%) in stoichiometry as given by the formula $Pr_{1-x}Sr_xFeAsO$. All the weighing and mixing procedures were performed in a glove box with a protective argon atmosphere. Then the mixtures were pressed into pellets and sealed in a quartz tube with an atmosphere of 20% Ar. The materials were heated up to 1150 °C with a rate of 120 °C/hr and maintained for 60 h. Then a cooling procedure was followed. It is important to note that the use of SrAs as the starting material, instead of using $SrCO_3$ or SrO, is very essential to synthesize the high quality samples, and to suppress the secondary impurity phases more. This new route makes our hole-doped samples easily reproduced.

The x-ray diffraction (XRD) measurements of our samples were carried out by a *Mac-Science* MXP18A-HF equipment with θ-2θ scan. The dc magnetization measurements were done with a superconducting quantum interference device [Quantum Design, superconducting quantum interference device (SQUID), MPMS7] and the ac susceptibility of the samples were measured on the Maglab-12T (Oxford) with an ac field of 0.1 Oe and a frequency of 333 Hz. The resistance and Hall-effect measurements were

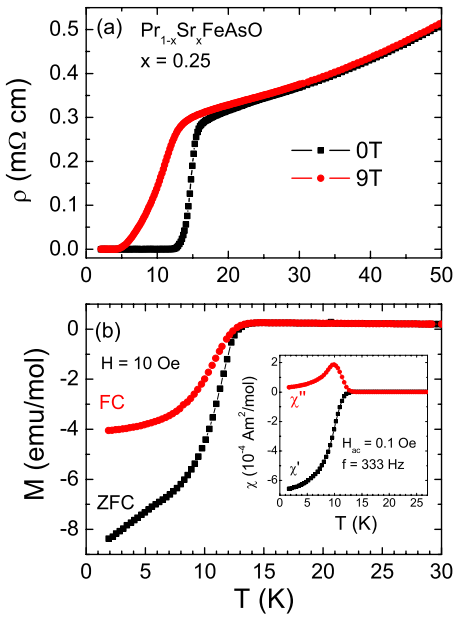

FIG. 1. (Color online) (a) Temperature dependence of resistivity for the $Pr_{0.75}Sr_{0.25}FeAsO$ sample under two different magnetic fields 0 and 9 T near the superconducting transition. A rather sharp transition can be seen at zero field. (b) Temperature dependence of dc magnetization for the zero-field cooling (ZFC) and field cooling (FC) process at $H=10$ Oe. The inset shows the ac susceptibility of the same sample measured with $H_{ac}=0.1$ Oe, $f=333$ Hz.

done using a six-probe technique on the Quantum Design instrument physical property measurement system (PPMS) with magnetic fields up to 9 T. The temperature stabilization was better than 0.1% and the resolution of the voltmeter was better than 10 nV.

III. EXPERIMENTAL DATA AND DISCUSSION

A. Resistive and diamagnetic transition

In Fig. 1(a) we present a typical set of resistive data for the sample $Pr_{1-x}Sr_xFeAsO$ with $x=0.25$ under 0 and 9 T near the superconducting transition. One can see that the resistivity transition at zero field is rather sharp indicating the quite high quality of our sample, and the onset transition temperature is about 16.3 K taking a criterion of 95% ρ_n. A magnetic field of 9 T only depresses the onset transition temperature about 2.5 K but makes the superconducting transition broader. The former behavior may indicate a rather high critical field in our sample, while the latter reflected the weak link between the grains.[19] Figure 1(b) shows the zero field cooled and also the field cooled dc magnetization of the same sample at 10 Oe. Moreover the diamagnetic transition measured with ac susceptibility technique is shown in the inset of Fig. 1(b). A rough estimate from the diamagnetic signal shows that the superconducting volume fraction of the present sample is beyond 50%, confirming the bulk superconductivity in our samples. The onset critical temperature by magnetic measurements is roughly corresponding to the zero resistivity temperature.

Shown in Fig. 2 is the temperature dependence of resistivity under zero field up to 300 K for the same sample as

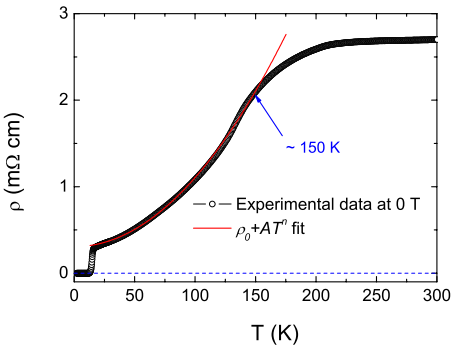

FIG. 2. (Color online) The resistivity curve at 0 T in the temperature region up to 300 K for the sample with $x=0.25$. A flattening of resistivity in high-temperature region is obvious, which seems to be a common feature of the hole-doped FeAs-based superconductors (Refs. 4, 15, and 16). The red solid line shows the fit below about 150 K using the formula $\rho=\rho_0+AT^n$.

shown in Fig. 1. The resistivity data in the normal state were fitted using the formula

$$\rho = \rho_0 + AT^n, \tag{1}$$

as we had done in the F-doped LaFeAsO system.[19] As represented by the red solid line in Fig. 2, the data below about 150 K can be roughly fitted with the fitting parameters $\rho_0=0.306$ mΩ cm and $n=2.000$. The fine quadratic dependent behavior of the resistivity, which is consistent with the prediction of the Fermi-liquid theory, may suggest a rather strong scattering between electrons in the present system in the low-temperature region. In a high-temperature region above about 150 K, however, a flattening of resistivity was observed clearly. The similar behavior has been observed in other hole-doped FeAs-1111 systems $La_{1-x}Sr_xFeAsO$ and $Nd_{1-x}Sr_xFeAsO$,[15–17] and also in the FeAs-122 system $(Ba,Sr)_{1-x}K_xFe_2As_2$.[4] We have pointed out that this behavior may be a common feature of the hole-doped FeAs-based superconductors.[16]

B. Doping dependence of lattice constants and superconducting properties

The XRD patterns for the samples with the nominal doping levels of 0.05~0.25 are shown in Fig. 3. Some small peaks from small amount of FeAs impurity phase which were denoted by red asterisks can still be seen, and the sample with $x=0.05$ has a bit more impurity phase FeAs than other samples. However, it is clear that all the main peaks can be indexed to the FeAs-1111 phase with the tetragonal ZrCuSiAs-type structure. By having a closer scrutiny one can find that the diffraction peaks shift slightly to the low-angle side when more strontiums are doped into the samples, suggesting an expanding effect of the lattice constants. The similar behavior has been observed in the Sr-doped LaFeAsO system previously.[16] By using the software of Powder-X,[20] we took a general fit to the XRD data of each sample and determined the lattice constants. The doping dependence of the lattice constants calculated from the XRD data, along with the data of the undoped and 11% F-doped

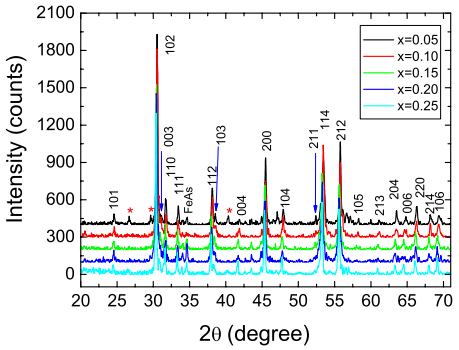

FIG. 3. (Color online) X-ray diffraction patterns for $Pr_{1-x}Sr_xFeAsO$ samples with different doping levels: x=0.05, 0.10, 0.15, 0.20, and 0.25. One can see that all the main peaks can be indexed to the tetragonal ZrCuSiAs-type structure. Small amount of impurity phases were denoted by red asterisks.

PrFeAsO samples,[11] are presented in Fig. 4. It is clear that both the a and c axes lattice constants expand monotonously from 11% F-doped PrFeAsO to the Sr-doped samples. This indicates that the strontium atoms go into the crystal lattice of the PrFeAsO system because the radii of Sr^{2+} (1.12 Å) is larger than that of Pr^{3+} (1.01 Å). It is worth noting that the extent of the lattice expanding is appreciably smaller than that in the Sr-doped LaFeAsO system, where the maximum onset transition temperature can be as high as 26 K.[15,16] In some cases, we see a slight drop of resistivity at temperatures as high as 28 K. So we believe that a further increase in T_c is possible if more strontium can be chemically doped into this system, like in the case of $Nd_{1-x}Sr_xFeAsO$.[17]

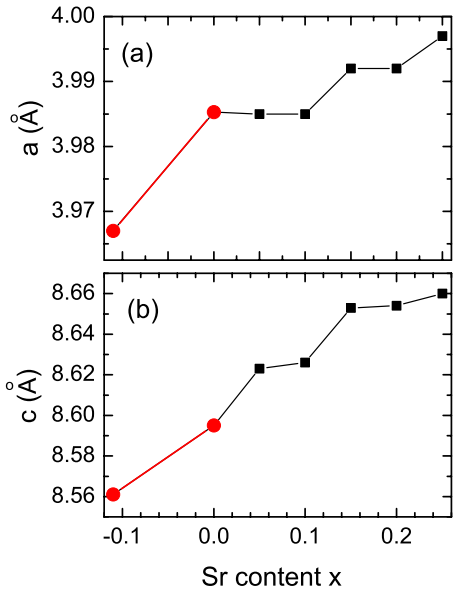

FIG. 4. (Color online) Doping dependence of (a) a-axis lattice constant; (b) c-axis lattice constant. The black filled squares represent data from our measurements. For electron-doped side, the variable "x" represents the fluorine concentration. The data of the undoped and F-doped cases (red filled circles) are taken from the work of Ren *et al.* (Ref. 11). One can see that the lattice constant roughly show a monotonous variation versus doping from electron doped region to hole-doped one.

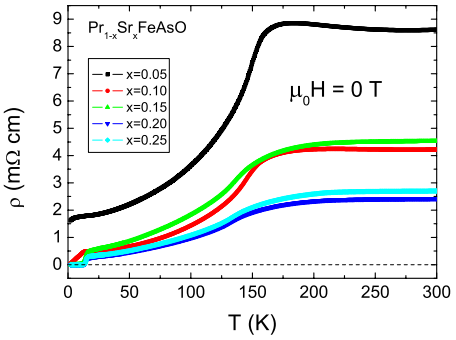

FIG. 5. (Color online) Temperature dependence of resistivity of samples $Pr_{1-x}Sr_xFeAsO$ with x=0.05, 0.10, 0.15, 0.20, and 0.25. One can see that the resistivity anomaly is suppressed gradually by doping more Sr into the system. The maximum onset transition temperature appears around the nominal doping level of 0.20 ~ 0.25.

In Fig. 5 we show the resistivity data of our samples made at various nominal doping levels of Sr ranging from x =0.05 to 0.25. A clear but rounded resistivity anomaly can be seen around 155 ~ 175 K when the doping level is 5%. Moreover a tiny resistivity drop at about 6 K which may be induced by the antiferromagnetic ordering of Pr^{3+} ions or superconductivity can be observed. At this time it is difficult to discriminate between the two scenarios since the magnitude of the resistivity drop is quite small. At the doping levels of 0.10 ~ 0.25, resistivity anomaly in the high-temperature regime is suppressed gradually and it eventually evolves into a flattening behavior at high doping levels. Also the magnitude of resistivity reduces obviously compared with the sample with 5% doping, suggesting that more and more conducting charge carriers were introduced into the samples. At the same time, the superconductivity emerges with doping and becomes optimal with an onset transition temperature of 16.3 K when the doping level is x=0.20 ~ 0.25. It is worth noting that the resistivity at high temperatures at a high doping level of holes behaves in a different way compared with that in the electron-doped samples[11,21,22] where the resistivity anomaly is suppressed completely and the resistivity always presents a metallic behavior in that regime. While in the hole-doped samples, the resistivity anomaly is smeared much slower.[15–17] In the $Nd_{1-x}Sr_xFeAsO$ system,[17] for example, it is found that the structural transition from tetragonal to orthorhombic occurs even in the sample with superconductivity. Doping more holes may lead to stronger suppression to the structural transition as well as the SDW order; this may leave a potential space to increase the superconducting transition temperature in the hole-doped FeAs-1111 phase.

C. Hall effect

It is known that for a conventional metal with Fermi-liquid feature, the Hall coefficient is almost independent of temperature. However, this situation is changed for a multi-band material[23] or a sample with non-Fermi liquid behavior, such as the cuprate superconductors.[24] To get more information about the conducting carriers, we measured the Hall

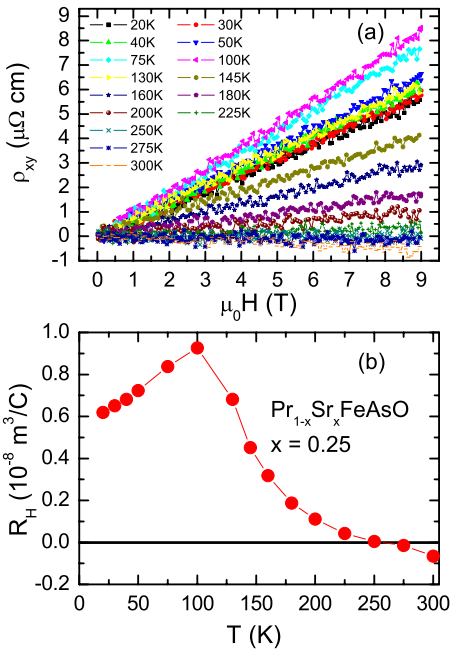

FIG. 6. (Color online) Hall-effect measurements for one sample $Pr_{0.75}Sr_{0.25}FeAsO$. (a) Hall resistivity ρ_{xy} versus the magnetic field $\mu_0 H$ at different temperatures. (b) Temperature dependence of the Hall coefficient R_H. A huge hump appears in the intermediate temperature region, which seems to be a common feature for the hole-doped FeAs-based superconductors.

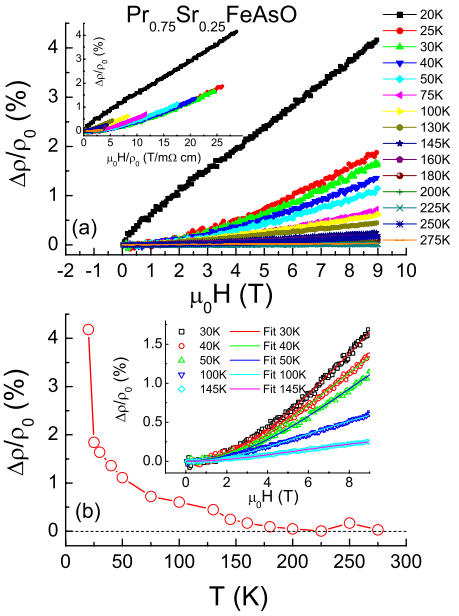

FIG. 7. (Color online) (a) Field dependence of MR $\Delta\rho/\rho_0$ at different temperatures for the sample with $x=0.25$. The inset shows Kohler plot of the same sample. It is clear that Kohler's rule is not obeyed. (b) Temperature dependence of MR for the same sample determined at 9 T. Shown in the inset is the theoretical fit to the field dependent MR data using a two-band model (see text).

effect of the sample with $x=0.25$ (the same one as shown in Fig. 1). Figure 6(a) shows the magnetic field dependence of Hall resistivity (ρ_{xy}) at different temperatures. In the experiment ρ_{xy} was taken as $\rho_{xy}=[\rho(+H)-\rho(-H)]/2$ at each point to eliminate the effect of the misaligned Hall electrodes. It is clear that all curves in Fig. 6(a) have good linearity versus the magnetic field. Moreover, ρ_{xy} is positive at all temperatures below 250 K giving a positive Hall coefficient $R_H=\rho_{xy}/H$, which actually indicates that hole type charge carriers dominate the conduction in the present sample.

The temperature dependence of R_H is shown in Fig. 6(b). Very similar to that observed in $La_{1-x}Sr_xFeAsO$ samples,[15,16] the Hall coefficient R_H reveals a huge hump in the intermediate temperature regime and the value of R_H decreases down to zero at about 250 K, then it becomes slightly negative above that temperature. Here we employ a simple two-band scenario with different types of carriers to interpret this behavior. We have known that for a two-band system in the low-field limit, the Hall coefficient R_H can be written as

$$R_H = \frac{\sigma_1^2 R_1 + \sigma_2^2 R_2}{(\sigma_1 + \sigma_2)^2}, \tag{2}$$

where σ_i $(i=1,2)$ is the conductance for different types of charge carriers in different bands, and $R_i=-1/n_i e$ represents the Hall coefficient for each type of carrier separately with n_i the concentration of the charge carriers for the different bands. We attribute the strong temperature dependence of R_H in the present system to the complicated variation of the conductance σ_i with temperature, which reflects mainly the temperature dependent behavior of the scattering relaxation time. Moreover the sign-changing effect of R_H may indicate the presence of two different types of charge carriers (electron and hole type) in the present system. The conductance σ_i of electronlike and holelike carriers may vary differently with temperature, and the electronlike carriers become dominant when the temperature is higher than about 250 K.

This simple two-band model is consistent with the MR data (will be addressed in Sec. III D). However, if there are two types of carriers in two bands, we may expect ρ_{xy} to be quadratic in magnetic field. The linear behavior in the $\rho_{xy} \sim H$ curve shown in Fig. 6(a) seems to be not agree with this scenario. So further measurements with higher magnetic fields are required.

D. Magnetoresistance

Magnetoresistance is a very powerful tool to investigate the electronic scattering process and the information about the Fermi surface.[23,25] Field dependence of MR, for the sample with $x=0.25$ at different temperatures is shown in the main frame of Fig. 7(a). Here MR was expressed as $\Delta\rho/\rho_0=[\rho(H)-\rho_0]/\rho_0$, where $\rho(H)$ and ρ_0 represent the longitudinal resistivity at a magnetic field H and that at zero field, respectively. One can see that the curve obtained at 20 K reveals a rather different feature compared with the data at temperatures above 25 K. Also the magnitude of MR (obtained at 9 T) at 20 K reached two times of that at 25 K giving a sharp drop in the $\Delta\rho/\rho_0 \sim T$ curve when increasing the temperature as revealed in the main frame of Fig. 7. We attribute this behavior to the presence of fluctuant superconductivity in the low-temperature region ($\sim$16.3–20 K). At

temperatures higher than 150 K, the value of MR vanishes to zero gradually.

As for the case in the moderate temperature region, the $\Delta\rho/\rho_0 \sim H$ curve reveals a clear nonlinear behavior. In the inset of Fig. 7(b) we present the data at five typical temperatures in this region. These data were then fitted based on a simple two-band model which gave the following formula:

$$\frac{\Delta\rho}{\rho_0} = \frac{(\mu_0 H)^2}{\alpha + \beta \times (\mu_0 H)^2}, \tag{3}$$

with α and β as the fitting parameters which were related to the conductances and mobilities for the charge carriers in two bands. The fitting results were shown by the solid lines in the inset of Fig. 7(b). It is clear that Eq. (3) can describe our data quite well. This argument can be further confirmed by seeing about the situation of the so-called Kohler plot. The semiclassical transport theory has predicted that the Kohler rule, which can be written as

$$\frac{\Delta\rho}{\rho_0} = F\left(\frac{\mu_0 H}{\rho_0}\right), \tag{4}$$

will be held if only one isotropic relaxation time is present in a single-band solid-state system.[26] Equation (4) means that the $\Delta\rho/\rho_0$ vs $\mu_0 H/\rho_0$ curves for different temperatures should be scaled to a universal curve if the Kohler rule is obeyed. The scaling based on the Kohler plot for the present sample is revealed in the inset of Fig. 7(a). An obvious violation of the Kohler rule can be seen on this plot. We attribute this behavior to the presence of a multiband effect in the present system.

Actually, theoretical research and angle-resolved photoemission spectroscopic (ARPES) studies have shown a rather complicated Fermi surface and energy-band structure in the FeAs-based superconductors. Our data from measuring the Hall effect and MR are consistent with these conclusions.

E. Upper critical field

Finally, we attempted to estimate the upper critical field of the sample with $x=0.25$ from the resistivity data. Temperature dependence of resistivity under different magnetic fields is shown in the main frame of Fig. 8. Similar to that found in the F-doped LaFeAsO polycrystalline samples,[19,27] the onset transition point, which reflects mainly the upper critical field in the configuration of H∥ab-plane, shifts more slowly than the zero resistivity point to low temperatures under fields. We take a criterion of 95% ρ_n to determine the onset transition points under different fields, which are presented by the blue open circles in the inset of Fig. 6. From these data we can roughly estimate the upper critical field of this sample based on the Ginzburg-Landau (GL) theory. The following equation have been extract from the GL theory and used successfully on other samples:[19,27,28]

$$H_{c2}(T) = H_{c2}(0)\frac{1-t^2}{1+t^2}, \tag{5}$$

where $t=T/T_c$ is the reduced temperature and $H_{c2}(0)$ is the upper critical field at zero temperature. Taking $T_c=16.3$ K

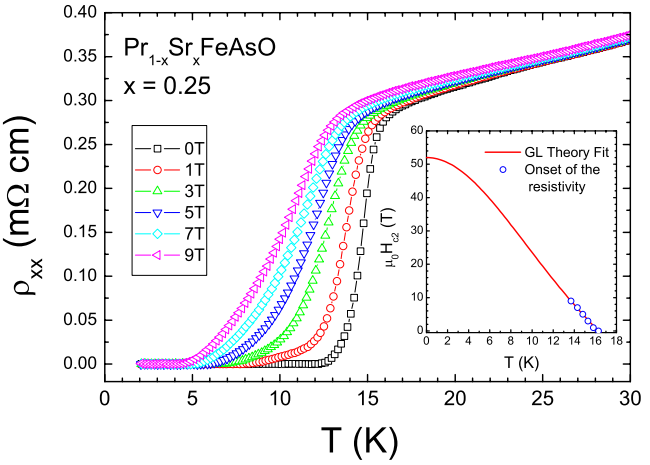

FIG. 8. (Color online) Temperature dependence of resistivity for the $Pr_{0.75}Sr_{0.25}FeAsO$ sample under different magnetic fields. The onset transition temperature defined by 95% ρ_n shifts with the magnetic field slowly. The inset shows the phase diagram derived from the resistive transition curves. The onset transition point is presented by the blue open circles. The red solid line shows the theoretical curve based on the GL theory [Eq. (5)].

and $H_{c2}(0)$ as the adjustable parameter, the measured data in the inset of Fig. 8 were then fitted using Eq. (5). One can see a quite good fit in the inset of Fig. 8 as revealed by the red solid line. The zero-temperature upper critical field was determined to be $H_{c2}(0) \approx 52$ T from the fitting process. Actually one can also determine the slope of $H_{c2}(T)$ near T_c, which is found to be about −4.0 T/K in the present sample. By using the WHH formula[18] the value of zero-temperature upper critical field $H_{c2}(0)$ can be estimated through

$$H_{c2}(0) = -0.693 T_c \left(\frac{dH_{c2}}{dT}\right)_{T=T_c}. \tag{6}$$

Taking $T_c=16.3$ K, we get $H_{c2}(0) \approx 45.1$ T. Regarding the relatively low value of $T_c=16.3$ K in the present sample, this value of upper critical field $H_{c2}(0)$ is actually quite high. The slope of $dH_{c2}(T)/dT|_{T_c}$ in the hole-doped sample is clearly larger than that in the electron-doped samples. In the hole-doped $La_{1-x}Sr_xFeAsO$ superconducting samples, we also found much larger $dH_{c2}(T)/dT|_{T_c}$ when comparing it with the F-doped LaFeAsO sample.[19,27] This may be understood as due to the higher quasiparticle density of states (DOS) near the Fermi level in the hole-doped samples. In a dirty type-II superconductor, it was predicted[29] that $-dH_{c2}/dT|_{T_c} \propto \gamma_n$ with γ_n the normal-state specific-heat coefficient which is proportional to the DOS at E_F. It is thus reasonable to ascribe the higher value of $dH_{c2}/dT|_{T_c}$ to higher DOS in the hole-doped samples. Theoretical calculations do show that the DOS in the hole-doped side is larger than that in the electron-doped samples.[30,31] The measurements on lower critical fields[32] and specific heat[33] in $Ba_{0.6}K_{0.4}Fe_2As_2$ reveal that the superfluid density and the normal-state DOS is about five to ten times larger than that in the F-doped REFeAsO system. If the normal-state DOS is really larger in the hole-doped systems, higher upper critical

fields may be achieved in the hole-doped FeAs-1111 samples provided that the superconducting transition temperature can be improved to the same scale.

IV. CONCLUDING REMARKS

In summary, bulk superconductivity was achieved by substituting Pr^{3+} with Sr^{2+} in PrFeAsO system. A systematic evolution of superconductivity and the lattice constants with doping in hole doped $Pr_{1-x}Sr_xFeAsO$ was discovered. By doping more Sr into the parent phase PrFeAsO, the anomaly of resistivity at about 165 K is suppressed gradually and the superconductivity eventually sets in. The *a* and *c* axes lattice constants increase monotonously with Sr concentration. The maximum superconducting transition temperature $T_c = 16.3$ K is found to appear around the nominal doping level $x = 0.20 \sim 0.25$. The positive Hall coefficient R_H in a wide temperature range suggests that the hole type charge carriers dominate the conduction in this system. The strong temperature dependence and sign-changing effect of R_H were attributed to a multiband effect and have been interpreted based on a simple two-band model with different types of charge carriers. This argument was further confirmed by the nonlinear field dependence of MR and the violation of the Kohler rule. Interestingly, the slope of the upper critical magnetic field vs temperature near T_c seems to be much higher than that of the electron-doped samples. This is attributed to the higher DOS in the hole-doped samples than in the electron-doped ones. This may provide a new way to enhance the upper critical field in the hole-doped FeAs-1111 superconductors.

ACKNOWLEDGMENTS

We acknowledge the help of XRD experiments from L. H. Yang and H. Chen. This work is supported by the Natural Science Foundation of China, the Ministry of Science and Technology of China (973 project: Grant Nos. 2006CB01000 and 2006CB921802), the Knowledge Innovation Project of Chinese Academy of Sciences (ITSNEM).

*hhwen@aphy.iphy.ac.cn

[1] Y. Kamihara, T. Watanabe, M. Hirano, and H. Hosono, J. Am. Chem. Soc. **130**, 3296 (2008).
[2] Hai-Hu Wen, Adv. Mater. (Weinheim, Ger.) **20**, 3764 (2008).
[3] R. Pottgen and D. Johrendt, Z. Naturforsch., B: Chem. Sci. **63B**, 1135 (2008).
[4] M. Rotter, M. Tegel, and D. Johrendt, Phys. Rev. Lett. **101**, 107006 (2008).
[5] K. Sasmal, B. Lv, B. Lorenz, A. M. Guloy, F. Chen, Y. Y. Xue, and C. W. Chu, Phys. Rev. Lett. **101**, 107007 (2008).
[6] X. C. Wang, Q. Q. Liu, Y. X. Lv, W. B. Gao, L. X. Yang, R. C. Yu, F. Y. Li, and C. Q. Jin, Solid State Commun. **148**, 538 (2008)
[7] Joshua H. Tapp, Zhongjia Tang, Bing Lv, Kalyan Sasmal, Bernd Lorenz, Paul C. W. Chu, and Arnold M. Guloy, Phys. Rev. B **78**, 060505(R) (2008).
[8] Michael J. Pitcher, Dinah R. Parker, Paul Adamson, Sebastian J. C. Herkelrath, Andrew T. Boothroyd, and Simon J. Clarke, Chem. Commun. (Cambridge) **2008**, 5918.
[9] X. H. Chen, T. Wu, G. Wu, R. H. Liu, H. Chen, and D. F. Fang, Nature (London) **453**, 761 (2008).
[10] G. F. Chen, Z. Li, D. Wu, G. Li, W. Z. Hu, J. Dong, P. Zheng, J. L. Luo, and N. L. Wang, Phys. Rev. Lett. **100**, 247002 (2008).
[11] Z.-A. Ren, J. Yang, W. Lu, W. Yi, G.-C. Che, X.-L. Dong, L.-L. Sun, and Z.-X. Zhao, Mater. Res. Innovations **12**, 105 (2008).
[12] Z. A. Ren, W. Lu, J. Yang, W. Yi, X. L. Shen, Z. C. Li, G. C. Che, X. L. Dong, L. L. Sun, F. Zhou, and Z. X. Zhao, Chin. Phys. Lett. **25**, 2215 (2008).
[13] P. Cheng, L. Fang, H. Yang, X. Zhu, G. Mu, H. Luo, Z. Wang, and H.-H. Wen, Sci. China, Ser. G **51**, 719 (2008).
[14] C. Wang, L. Li, S. Chi, Z. Zhu, Z. Ren, Y. Li, Y. Wang, X. Lin, Y. Luo, S. Jiang, X. Xu, G. Cao, and X. Zhu'an, Europhys. Lett. **83**, 67006 (2008).
[15] H. H. Wen, G. Mu, L. Fang, H. Yang, and X. Y. Zhu, Europhys. Lett. **82**, 17009 (2008).
[16] G. Mu, L. Fang, H. Yang, X. Zhu, P. Cheng, and H.-H. Wen, J. Phys. Soc. Jpn. **77**, 15 (2008).
[17] K. Kasperkiewicz, J.-W. G. Bos, A. N. Fitch, K. Prassides, and S. Margadonna, Chem. Commun. (Cambridge) **2009**, 707.
[18] N. R. Werthamer, E. Helfand, and P. C. Hohenberg, Phys. Rev. **147**, 295 (1966).
[19] X. Zhu, H. Yang, L. Fang, G. Mu, and H.-H. Wen, Supercond. Sci. Technol. **21**, 105001 (2008).
[20] C. Dong, J. Appl. Crystallogr. **32**, 838 (1999).
[21] J. Dong, H. J. Zhang, G. Xu, Z. Li, G. Li, W. Z. Hu, D. Wu, G. F. Chen, X. Dai, J. L. Luo, Z. Fang, and N. L. Wang, Europhys. Lett. **83**, 27006 (2008).
[22] Y. Jia, P. Cheng, L. Fang, H. Luo, H. Yang, C. Ren, L. Shan, C. Gu, and H.-H. Wen, Appl. Phys. Lett. **93**, 032503 (2008).
[23] H. Yang, Y. Liu, C. G. Zhuang, J. R. Shi, Y. G. Yao, S. Massidda, M. Monni, Y. Jia, X. X. Xi, Q. Li, Z. K. Liu, Q. R. Feng, and H. H. Wen, Phys. Rev. Lett. **101**, 067001 (2008).
[24] T. R. Chien, D. A. Brawner, Z. Z. Wang, and N. P. Ong, Phys. Rev. B **43**, 6242 (1991).
[25] Q. Li, B. T. Liu, Y. F. Hu, J. Chen, H. Gao, L. Shan, H. H. Wen, A. V. Pogrebnyakov, J. M. Redwing, and X. X. Xi, Phys. Rev. Lett. **96**, 167003 (2006).
[26] J. M. Ziman, *Electrons and Phonons, Classics Series* (Oxford University Press, New York, 2001).
[27] G. F. Chen, Z. Li, G. Li, J. Zhou, D. Wu, J. Dong, W. Z. Hu, P. Zheng, Z. J. Chen, H. Q. Yuan, J. Singleton, J. L. Luo, and N. L. Wang, Phys. Rev. Lett. **101**, 057007 (2008).
[28] L. Fang, Y. Wang, P. Y. Zou, L. Tang, Z. Xu, H. Chen, C. Dong, L. Shan, and H. H. Wen, Phys. Rev. B **72**, 014534 (2005).
[29] J. E. Jaffe, Phys. Rev. B **40**, 2558 (1989).
[30] D. J. Singh, Phys. Rev. B **78**, 094511 (2008).
[31] F. Ma, Z.-Y. Lu, and T. Xiang, arXiv:0806.3526 (unpublished).
[32] C. Ren, Z. Wang, H. Luo, H. Yang, L. Shan, and H.-H. Wen, Phys. Rev. Lett. **101**, 257006 (2008)
[33] G. Mu, H. Luo, Z. Wang, L. Shan, C. Ren, and H.-H. Wen, arXiv:0808.2941 (unpublished).